

SMR 1232 - 12

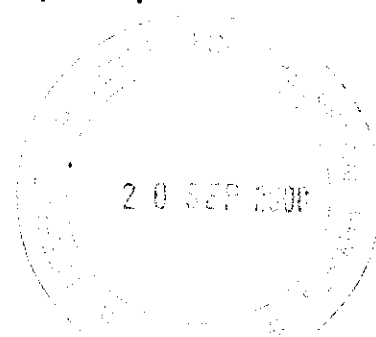
**XII WORKSHOP ON
STRONGLY CORRELATED ELECTRON SYSTEMS**

17 - 28 July 2000


Overview of Transport Models in Cuprates

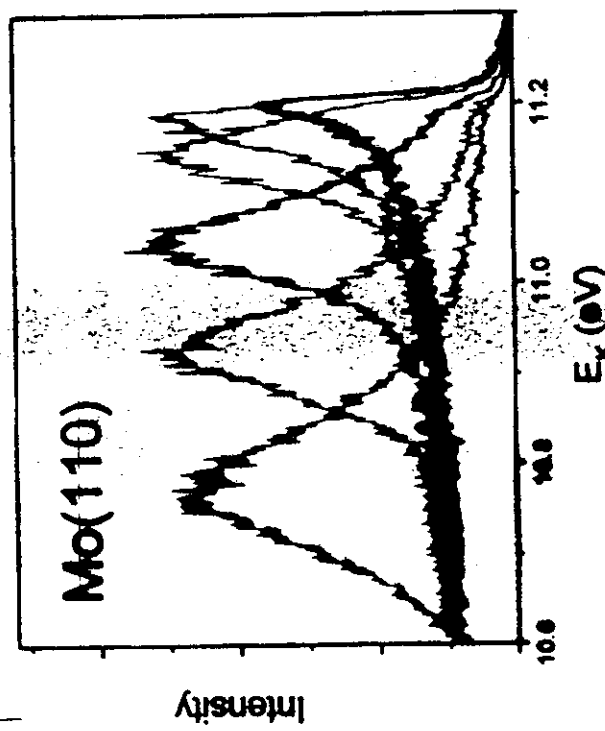
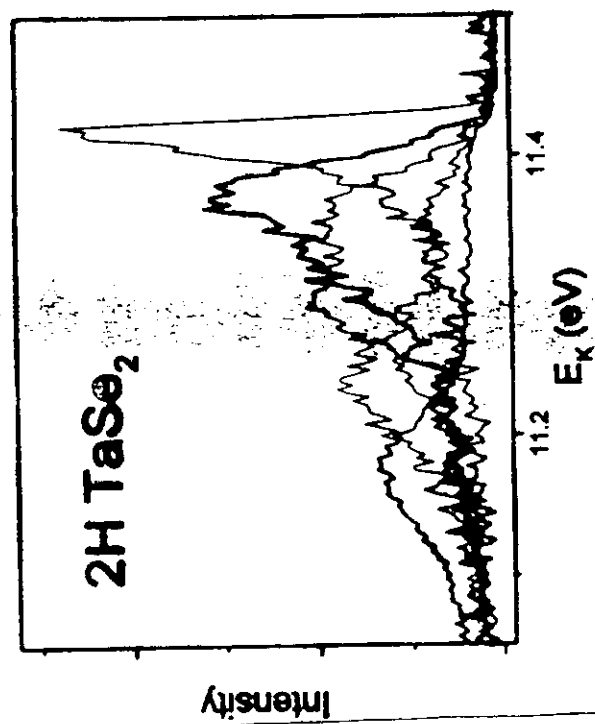
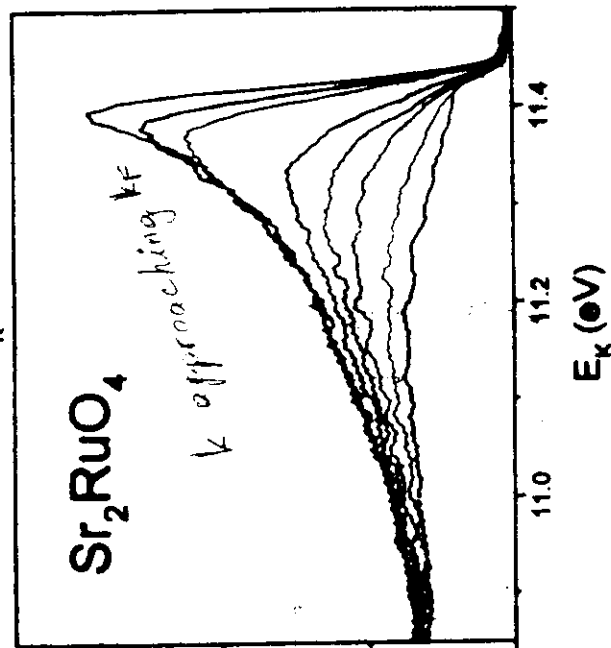
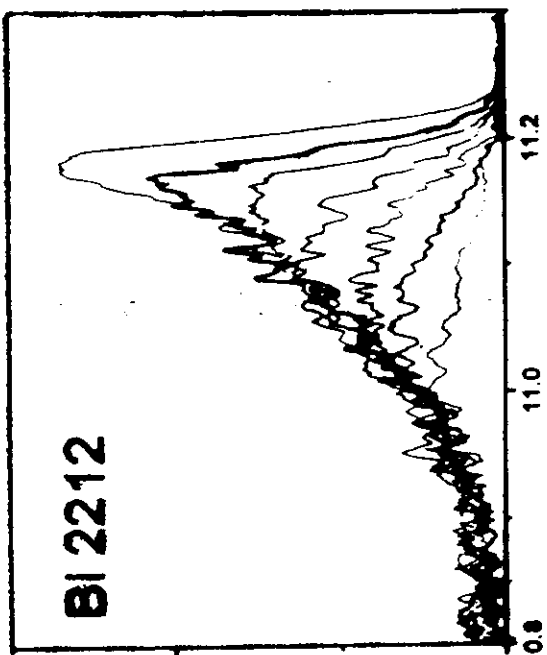
Victor YAKOVENKO
University of Maryland, College Park, MD, U.S.A.

These are preliminary lecture notes, intended only for distribution to participants.



Undisputable facts about cuprates (in the normal state)

- 1) Fermi surface does exist and has been very well measured by photoemission.
 - The shape of FS is best obtained by MDCs (momentum distribution curves). 
 - The shape of EDCs (energy distribution curves) is abnormal.
- 2) Different parts of the Fermi surface have different properties: (π, π) vs $(\pi, 0)$
 - scattering rates
 - spectral weights
 - pseudogap
- 3) It is not possible to fit the transport data with a single relaxation time τ (à la Drude).
 - $\sigma_{xx}(T) \propto \tau(T) \propto \frac{1}{T}$; $\sigma_{xy} \propto \tau^2 \sim \frac{1}{T^3}$
 - $\sigma_{xx}(\omega)$, $\sigma_{xy}(\omega)$: Drew's group, PRL 1996
 - At least two (or more) relaxation times are required.



From Peter Johnson (BNL)

tivity that falls off as with frequency as ω^{-1} (with logarithmic corrections), more slowly than the ω^{-2} dependence of the familiar Drude form; a Raman scattering intensity $\propto \max(\omega, T)/T$; a T -independent contribution to the copper nuclear spin relaxation rate; and (in some geometries) a linear in bias voltage contribution to the single-particle tunneling rate. The MFL phenomenology has often been used to fit experiments, and it is found that the behavior of response functions is generally consistent with MFL as expressed in Eq. 1.

Nevertheless, although there were some direct indications of the correctness of Eq. 2 in early ARPES measurements (5), the MFL behavior of the single-particle excitation spectrum [i.e., Eq. 2] was not adequately confirmed. ARPES experiments measure the single-particle properties directly, in contrast to response functions, which are governed by joint two-particle (that is, particle-hole) properties. The quantity determined in ARPES experiments is the single-particle spectral function $\mathcal{A}(\mathbf{k}, \omega)$, which depends on the self energy as follows:

$$\mathcal{A}(\mathbf{k}, \omega) = \frac{1}{\pi} \frac{\Sigma_2(\mathbf{k}, \omega)}{[\omega - \varepsilon_{\mathbf{k}} - \Sigma_1(\mathbf{k}, \omega)]^2 + [\Sigma_2(\mathbf{k}, \omega)]^2} \quad [3]$$

The MFL behavior of the single-particle excitations has now been verified convincingly in the new ARPES experiments of Valla *et al.* (6) at Brookhaven National Laboratory and by Kaminski *et al.* (7) at Argonne National Laboratory. In the past, such measurements have been limited by energy and momentum resolution and large experimental backgrounds in the energy distribution measurements at fixed momentum (EDCs). These problems are now being overcome as new detectors have come on line. In particular, Valla *et al.* (6) have taken advantage of improved resolution to measure, on optimally doped $\text{Bi}_2\text{Sr}_2\text{CaCu}_2\text{O}_{8+\delta}$, in addition to EDCs, momentum distributions at fixed energy (MDCs). In this way, the frequency dependence of the single-particle spectral function $\mathcal{A}(\mathbf{k}, \omega)$ is measured at fixed \mathbf{k} (EDC) and also the \mathbf{k} dependence at fixed ω (MDC).

It follows from Eq. 3 that, if the self energy Σ is momentum independent perpendicular to the Fermi surface, then an MDC scanned along \mathbf{k}_{perp} for $\omega \approx 0$ should have a lorentzian shape plotted against $(\mathbf{k} - \mathbf{k}_F)_{\text{perp}}$ with a width proportional to $\Sigma_2(\omega)$, and the Σ_2 found in this way from MDCs should agree with that found by fitting EDCs. Furthermore, for an MFL, the width should be proportional to $x = \max(|\omega|, T)$, where ω is measured from the chemical potential. This behavior has now been verified by Valla *et al.* (6). The fits of the MDCs at $\omega = 0$ to a lorentzian are shown in Fig. 1A. Fig. 1B shows the linear variation of the width of the lorentzian with temperature.

Preliminary data from both the Brookhaven (8) and Argonne (A. Kaminski, personal communication) groups also show that the contribution to Σ_2 , which is proportional to x as determined by scans perpendicular to the Fermi surface, is very weakly dependent on \mathbf{k}_F ; i.e., it varies only weakly with the angle on the Fermi surface. It is important to notice that there is no evidence of a T^2 contribution to Σ_2 in the neighborhood of the Fermi surface anywhere in the Brillouin zone; the temperature-dependent part is always T linear.

Phenomenological ideas that seek to explain the transport anomalies in the cuprates on the basis of hot and cold spots on the Fermi surface are not consistent with this experimental finding, because they are based on having a T^2 behavior in the (1,1) direction and a T behavior in the (1,0) direction.

The Argonne group has plotted the EDCs together with fits to the MFL spectral function of Eq. 3 at over a dozen \mathbf{k} -points between the (1,1) and (1,0) directions in the Brillouin zone. $\text{Im}\Sigma(\omega)$ is taken to be of the form $\Gamma(\mathbf{k}) + \lambda(\mathbf{k}_F)\omega$. Γ represents an impurity contribution (see below). We show two typical examples in Fig. 2A and B. These display, respectively, the results

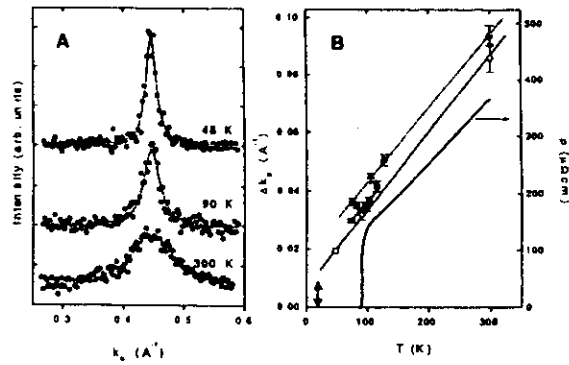


Fig. 1. (A) Momentum distribution curves for different temperatures. The solid lines are Lorentzian fits. (B) Momentum widths of MDCs for three samples (circles, squares, and diamonds). The thin lines are T -linear fits. The resistivity (solid black line) is also shown. The double-headed arrow shows the momentum resolution of the experiment. Figure courtesy of P. D. Johnson (Brookhaven National Laboratory). Reproduced with permission from ref. 6 (Copyright 1999, American Association for the Advancement of Science).

at the Fermi surface in the (1,0) and the (1,1) directions in the Brillouin zone that give the widest \mathbf{k} variations of Γ and λ . These self-energy parameters for the fit are given in the legend to Fig. 2.

Thus, the results for MDCs as well as EDCs may be summarized by the following expression:

$$\Sigma_2(\mathbf{k}, \omega; T) \equiv \Gamma(\mathbf{k}_F) + \Sigma_2^{\text{MFL}}(\omega; T). \quad [4]$$

The first term on the right-hand side of Eq. 3 is independent of frequency and temperature and is properly considered as the scattering rate because of static impurities. This can depend on \mathbf{k}_F , the direction of \mathbf{k} around the Fermi surface, as explained below. The second term is the MFL self energy of Eq. 2, a function only of $x = \max(|\omega|, T)$; however a weak dependence on \mathbf{k} is possible, as discussed earlier. There may be additive analytic contributions of the normal Fermi-liquid type as well.

The dependence of the impurity scattering on \mathbf{k}_F can be understood by the assumption that in well-prepared cuprates, the impurities lie between the CuO_2 planes and therefore give rise

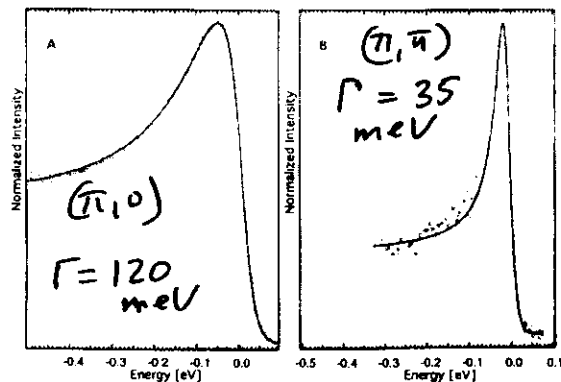


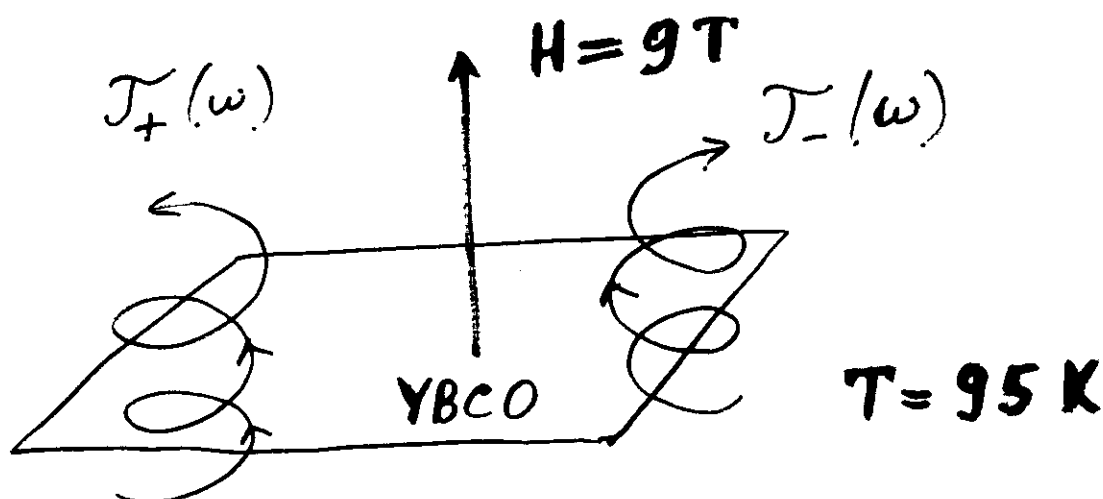
Fig. 2. Fits of the MFL self energy $\Gamma + \lambda\Delta\omega$ to the experimental data. Energies are in meV, with estimated uncertainties of $\pm 15\%$ in Γ and $\pm 25\%$ in λ . (A) The (1,0) direction, $\Gamma = 0.12$, $\lambda = 0.27$, and (B) the (1,1) direction, $\Gamma = 0.035$, $\lambda = 0.35$. Figure courtesy of A. Kaminski (Argonne National Laboratory). [Figure courtesy of A. Kaminski (Argonne National Laboratory), used by permission.]

$$\text{Im}\Sigma = \Gamma(\mathbf{k}) + \lambda(\mathbf{k})\omega$$

Σ_2

ac magnetotransport in $\text{YBa}_2\text{Cu}_3\text{O}_7$

Kaplan et al., Phys. Rev. Lett. 76, 696 (1996)



$$\frac{\sigma_{xx}(\omega)}{\sigma_{xy}(\omega)} \Rightarrow \cot \theta_H(\omega) = \sigma_{xx}(\omega) / \sigma_{xy}(\omega)$$

$$R_H(\omega) = \sigma_{xy}(\omega) / H \sigma_{xx}^2(\omega)$$

Simple Drude model:

$$\sigma_{xx}(\omega) \propto \tilde{\tau}(\omega) \omega_p^2$$

$$\sigma_{xy}(\omega) \propto \tilde{\tau}^2(\omega) \omega_p^2 \omega_H$$

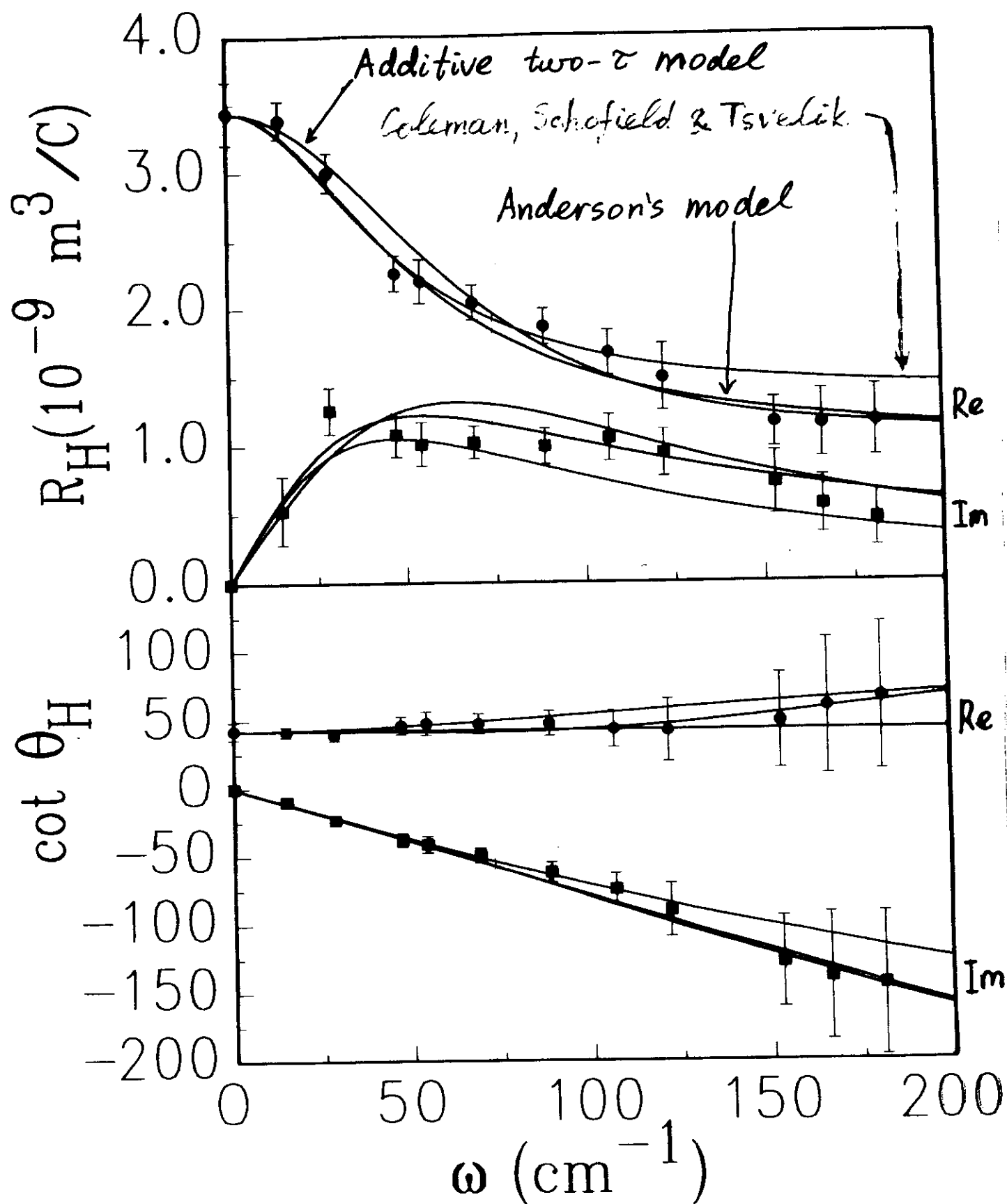
where $\frac{1}{\tilde{\tau}(\omega)} = \frac{1}{\tau} - i\omega$

$$\cot \theta_H(\omega) = \frac{1}{\omega_H \tilde{\tau}(\omega)} = \frac{\left(\frac{1}{\tau} - i\omega\right)}{\omega_H}$$

agrees with experiment

$R_H(\omega) = \text{const}(\omega)$ does not agree with experiment

$$\propto \frac{\omega_H}{\omega_p^2}$$



Transport models

1) Single- τ models

- Marginal Fermi liquid

Varma et al., PRL 1989

$$\rho_{xx} \propto \frac{1}{\tau} \propto \text{Im } \Sigma \propto \max(T, \omega)$$

- Luttinger liquid (Anderson, PRB 1997,

$$\sigma_{xx}(\omega) = \frac{A}{\left(\frac{1}{\tau} - i\omega\right)^\alpha}; \quad \frac{\text{Im } \sigma_{xx}(\omega)}{\text{Re } \sigma_{xx}(\omega)} \approx \text{const at } \omega \gg \frac{1}{\tau}$$

↑ Do not give predictions about $\sigma_{xy}(T, \omega)$

- Holon-spinon fluid

D.K. Lee & P.A. Lee, J. Phys. Cond. Mat. 1997

$$\omega_H \propto \frac{1}{T}; \quad \theta_H = \frac{\omega_H(T)}{\frac{1}{\tau} - i\omega}$$

- Skew scattering $\propto \frac{1}{T}$

Kotliar, Sengupta, Varma, PRB 1996

↑ Unsatisfactory because give $R_H(\omega) = \text{const}$

2) Global two- τ models

- Multiplicative model

Anderson; Ong, PRL, 1991

$$\sigma_{xx} \propto \tau_{tr} \propto \frac{1}{T}$$

$$\sigma_{xy} \propto \tau_{tr} \tau_H \propto \frac{1}{T^3}, \text{ where } \tau_H \propto \frac{1}{T^2}$$

For $\omega \neq 0$: $\frac{1}{\tilde{\tau}_{tr,H}} = \frac{1}{\tau_{tr,H}} - i\omega$

Drew et al.
PRL 1996

- Charge-conjugation model

Coleman, Schofield, Tsvelik, PRL 1996

$$\hat{C} \hat{\psi} = \pm \hat{\psi} \quad (\text{normally } \hat{C} \hat{\psi} = \hat{\psi}^+)$$

$$\text{relaxation rates } \Gamma_f \propto T \text{ \& } \Gamma_s \propto T^2$$

$$\rho_{xy} \propto \Gamma_f \Gamma_s \propto T^3; \rho_{xx} \propto (\Gamma_f + \Gamma_s) \propto T + T^2$$

3) Variation of τ over the Fermi surface.

- Additive two- τ model

Carrington, Mackenzie, Lin, Cooper, PRL 1992

Kendziora, Mandrus, Mihaly, Forro, PRB 1992

$$\sigma_{xx}(T), \sigma_{xy}(T)$$

Zheleznyak, Yakovenko, Drew, PRB 1998, 1999

$$\sigma_{xx}(\omega), \sigma_{xy}(\omega); \Delta\sigma_{xx}(H, T)$$

- Antiferromagnetic fluctuations

Klubina, Rice, PRB 1995

Stojković, Pines, 1996 - 1997

- Cold spots

Ioffe, Millis, PRB 1998

$$\frac{1}{\tau} = \frac{1}{\tau_0} + \Gamma k_t^2, \quad \frac{1}{\tau_0} \propto T^2, \quad \Gamma = \text{const}$$

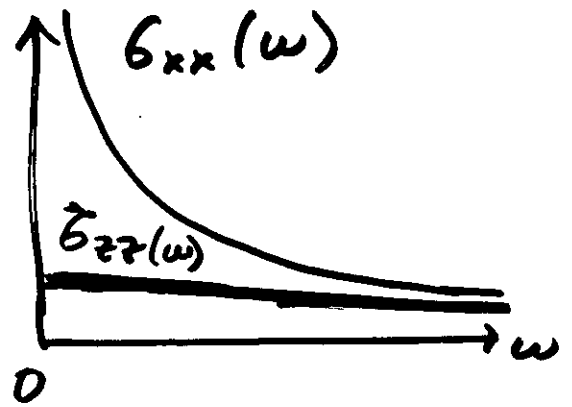
van der Marel, PRB 1999

$$\frac{1}{\tau} = \frac{1}{\tau_0} + \Gamma \sin^2(2\theta)$$

$$\sigma_{xx} \propto \frac{1}{\sqrt{\frac{1}{\tau_0} - i\omega}} \frac{1}{\sqrt{\frac{1}{\tau_0} + \Gamma - i\omega}} \propto \begin{cases} \frac{1}{\sqrt{-i\omega}}, & \frac{1}{\tau_0} \ll \omega \ll \Gamma \\ \frac{1}{-i\omega}, & \Gamma \ll \omega \end{cases}$$

$$t_{\perp} = t_0 \sin^2(2\theta)$$

$$\sigma_{zz} \propto \langle \tau(\theta) t_{\perp}^2(\theta) \rangle_{\theta}$$



Xiang, Hardy, cond-mat/0001443

$\sigma_{zz} \sim T^3$ in the superconducting state

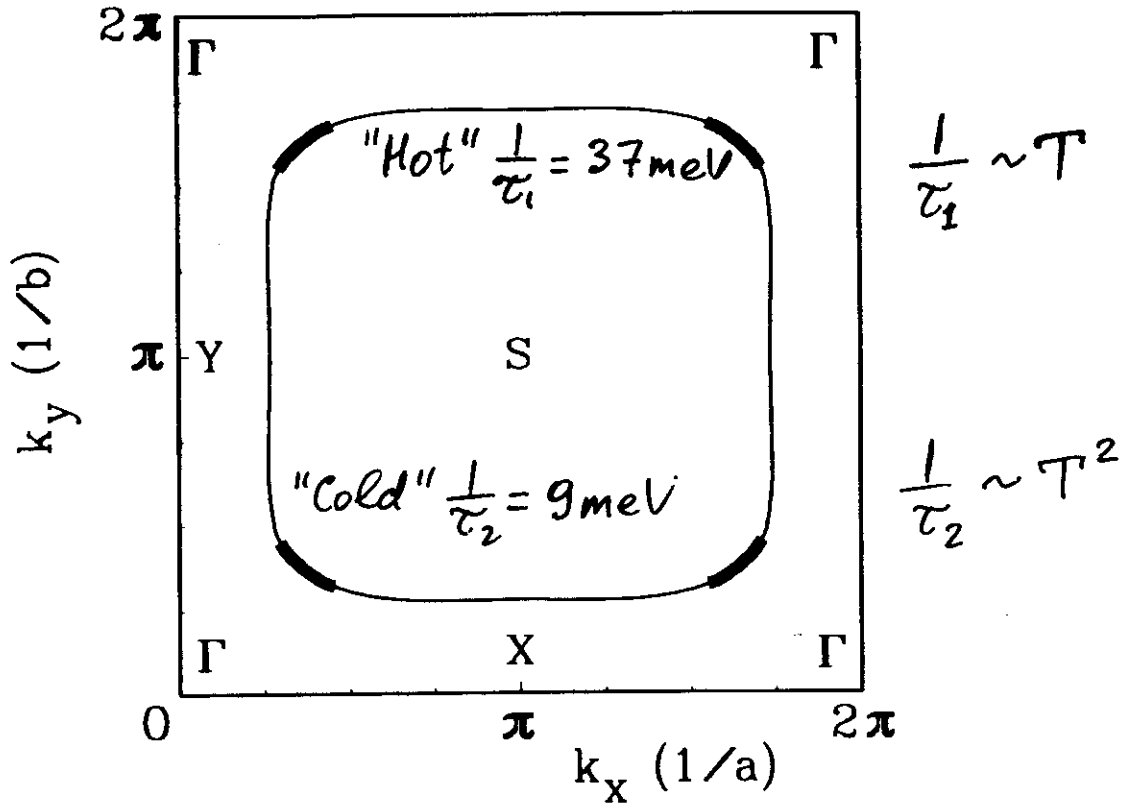
Corson, Drenstein et al, cond-mat/0006027

$$\phi(\tau) = \arg(\sigma_{xx}) \approx \frac{\text{Im } \sigma_{xx}}{\text{Re } \sigma_{xx}} \propto \omega \tau \sim \frac{1}{T^2}$$

(at small ω)

Zheleznyak, Yakovenko, Drew, Mazin
PRB 57, 3089 (1998)

Additive two- τ model



$$\sigma_{xx}(\omega) = A_1 \tilde{\tau}_1(\omega) + A_2 \tilde{\tau}_2(\omega)$$

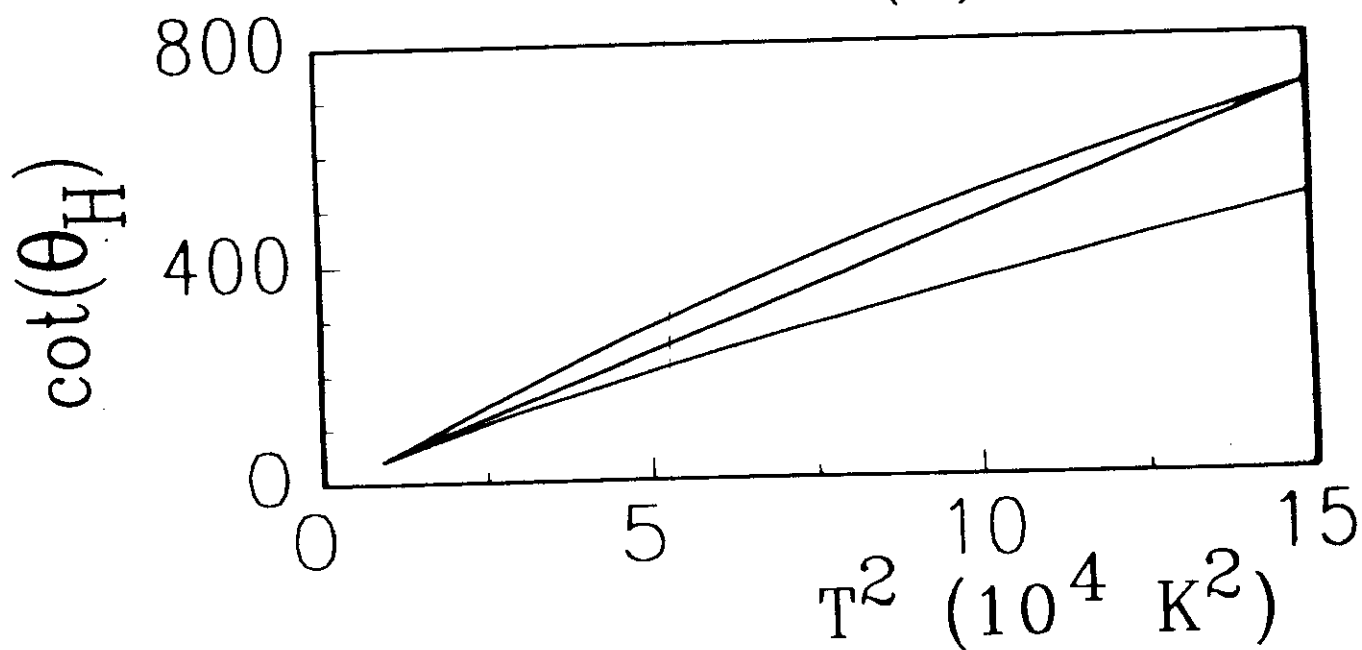
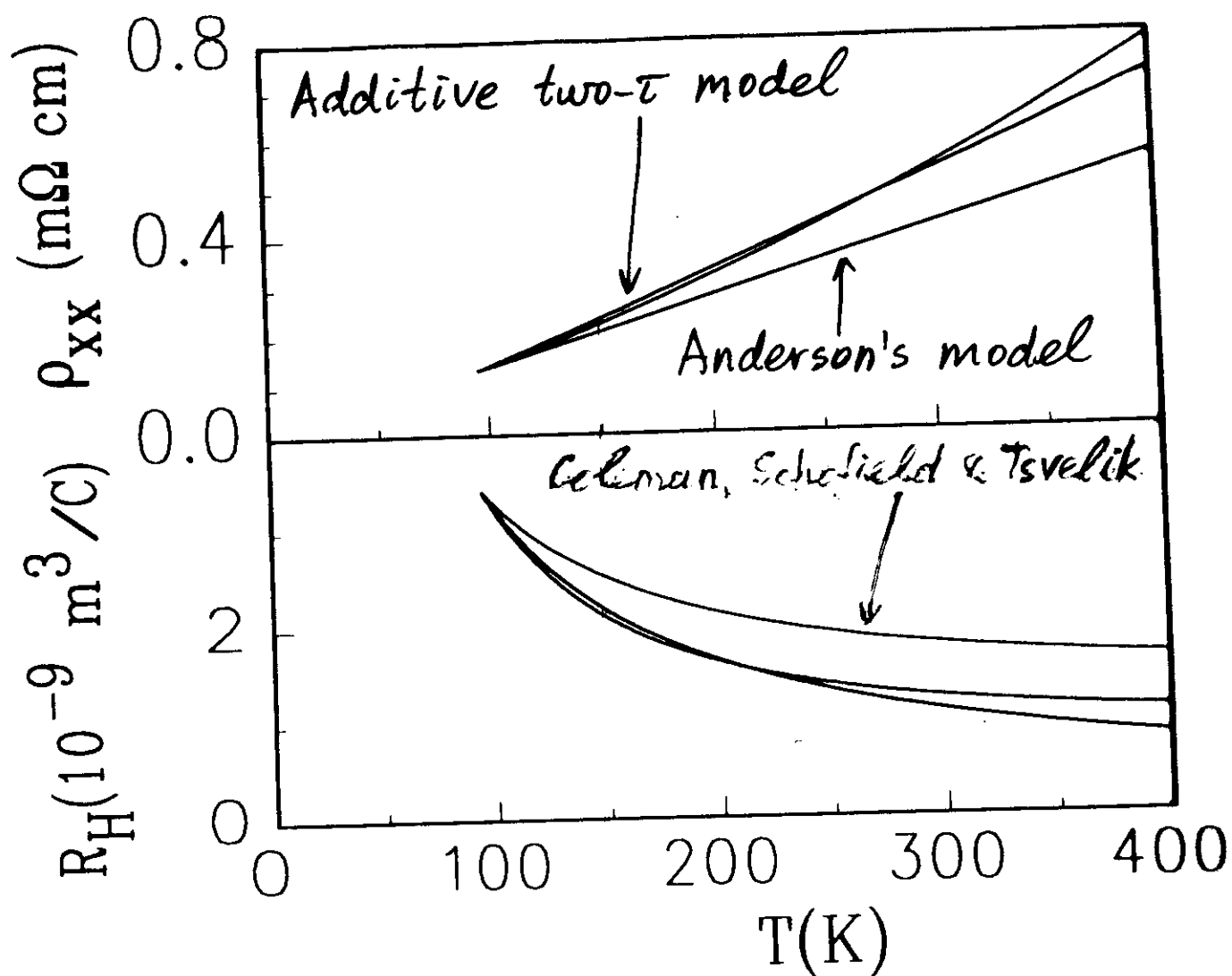
$$\sigma_{xy}(\omega) = B_1 \tilde{\tau}_1^2(\omega) + B_2 \tilde{\tau}_2^2(\omega)$$

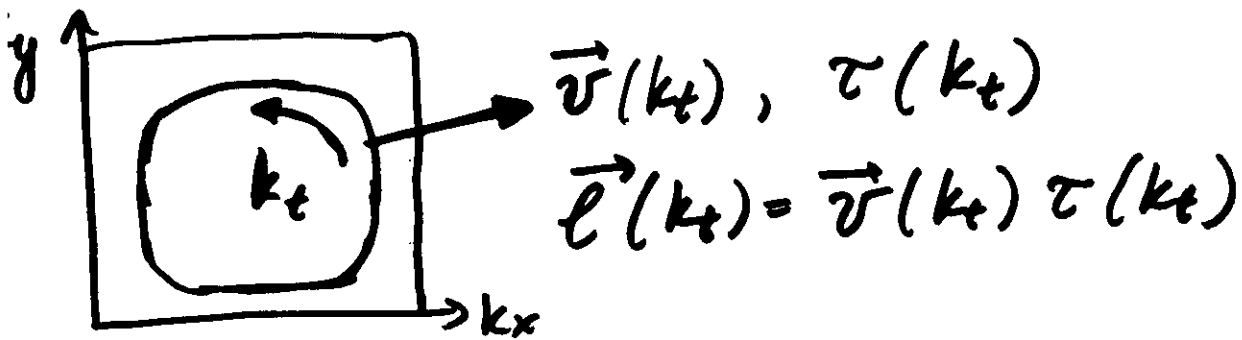
$$1/\tilde{\tau}_{1,2}(\omega) = 1/\tau_{1,2} - i\omega, \quad \tau_2/\tau_1 = 4$$

where

$$A_{1,2} \propto \int_{1,2} v(k_t) dk_t, \quad A_1 : A_2 = 9 : 1$$

$$B_{1,2} \propto \int_{1,2} \mathbf{v}(k_t) \times d\mathbf{v}(k_t), \quad B_1 : B_2 = 7 : 3$$





Conductivity:

$$\sigma_{xx}^{(0)} = \frac{e^2}{(2\pi)^2 \hbar d} \oint dk_t l(k_t)$$

Hall conductivity:

$$\sigma_{xy} = \frac{e^3 H}{(2\pi)^2 \hbar^2 c d} \oint \mathbf{e}_z \cdot [\mathbf{l}(k_t) \times d\mathbf{l}(k_t)]$$

Ong, PRB 1991

Magnetoconductivity: $\sigma_{xx}^{(2)} = \sigma_{xx}(H) - \sigma_{xx}(0)$

$$\begin{aligned} \sigma_{xx}^{(2)} &= \frac{2e^4 H^2}{(2\pi)^2 \hbar^3 c^2 d} \oint dk_t l_x(k_t) \frac{d}{dk_t} \left(l(k_t) \frac{dl_x(k_t)}{dk_t} \right) \\ &= -\frac{2e^4 H^2}{(2\pi)^2 \hbar^3 c^2 d} \oint dk_t l(k_t) \left(\frac{dl_x(k_t)}{dk_t} \right)^2 \end{aligned}$$

Harris, Ong, Anderson et al. PRL 1995

Zheleznyak, Yakovenko, Drew
PRB 59, 207 (1999)

Two- τ model with a transition zone

$$\tau(k_t) = \frac{\tau_1 + \tau_2}{2} \mp \frac{\tau_1 - \tau_2}{2} \tanh\left(\frac{k_t - \tilde{k}_t}{\kappa}\right)$$

$$\sigma_{xx}^{(2)} = -C_1\tau_1^3 - C_2\tau_2^3 - \tilde{\sigma}_{xx}^{(2)}$$

$$C_{1,2} = \frac{2e^4 H^2}{(2\pi)^2 \hbar^3 c^2 d} \int_{1,2} dk_t v(k_t) \left(\frac{dv_x(k_t)}{dk_t} \right)^2$$

$$\tilde{\sigma}_{xx}^{(2)} = \frac{2e^4 H^2}{(2\pi)^2 \hbar^3 c^2 d} v^3(\tilde{k}_t) \frac{(\tau_1 + \tau_2)(\tau_1 - \tau_2)^2}{6\kappa}.$$

Hall angle:

$$\tan \theta_H = \frac{\sigma_{xy}}{\sigma_{xx}^{(0)}}$$

Magnetoresistance:

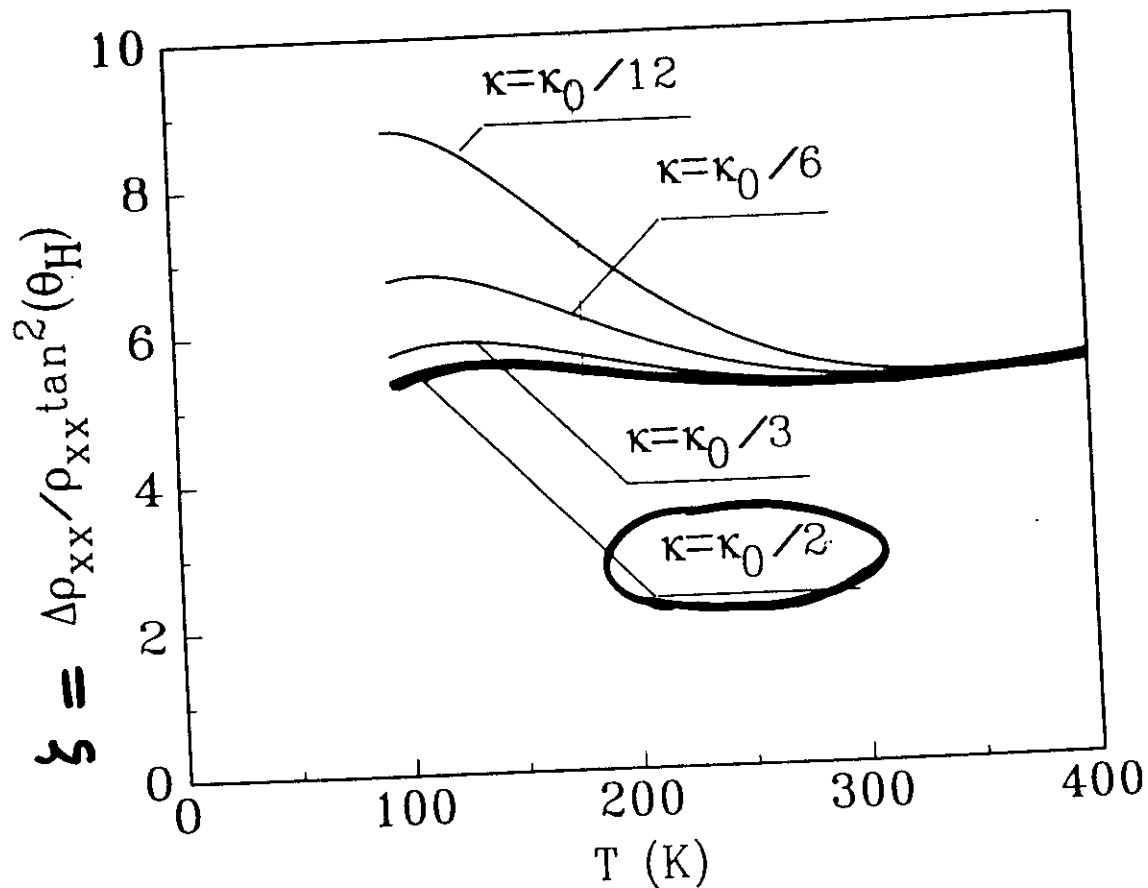
$$\frac{\Delta \rho_{xx}}{\rho_{xx}} = -\frac{\sigma_{xx}^{(2)}}{\sigma_{xx}^{(0)}} - \tan^2 \theta_H$$

$$\zeta = \frac{\Delta \rho_{xx}}{\rho_{xx} \tan^2 \theta_H} = -\frac{\sigma_{xx}^{(2)} \sigma_{xx}^{(0)}}{\sigma_{xy}^2} - 1$$

$$\bar{\zeta} = \frac{\oint dk_t v(k_t) (dv_x(k_t)/dk_t)^2 \oint dk_t v(k_t)}{2(\oint dk_t v_x(k_t) dv_y(k_t)/dk_t)^2} - 1 = 5.67$$

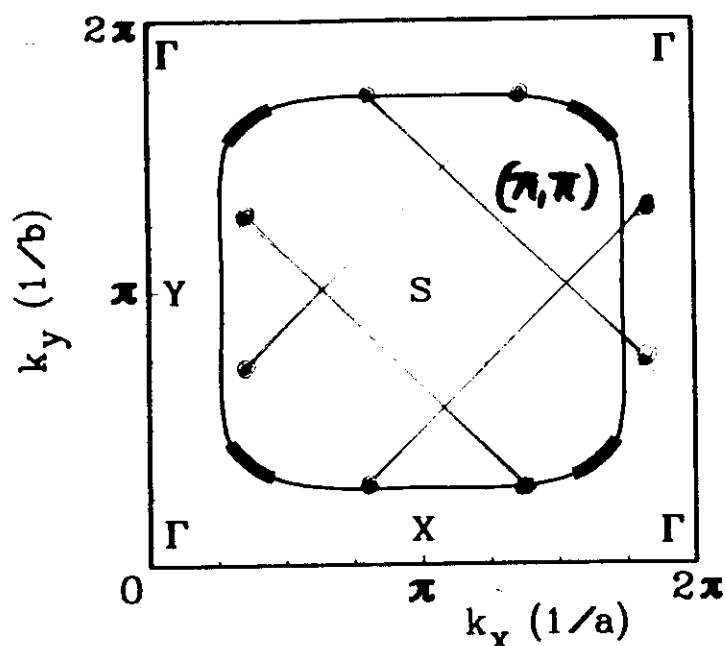
YBCO
band
structure

$\zeta = 1.5-1.7$ YBCO } Harris, Ong et al PRL 1995
 13.6 LSCO }
 3.6 optimally doped TlBaCuO } Tyler, McKenzie, Schofield 1998
 2.0 over



Dimensionless ratio of magnetoresistance and the Hall angle squared, $\Delta\rho_{xx}/\rho_{xx} \tan^2 \theta_H$, as a function of temperature for different values of κ .

Possible origins of the “cold spots”



1. Geometry of the Fermi surface: the sides of the square vs the corners, flat regions vs rounded, 1D vs 2D.
2. Fluctuations of a *d*-wave order parameter (superconducting or insulating): connection to the pseudogap.
3. Antiferromagnetic fluctuations at the wave vector (π, π) , via merger of the eight “hot spots”.

Qualitative arguments in favor of the “cold spots” model

1. Photoemission observes well-defined electron quasiparticles at the “cold spots” (α), but very broad excitations at the “hot” regions (β).

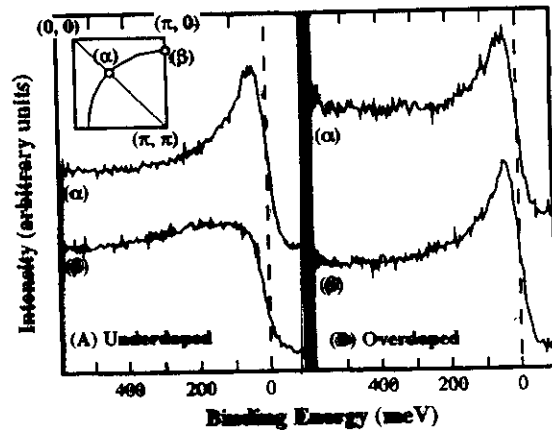


FIG. 1. ARPES data from an underdoped Bi2212 (A) and an overdoped Bi2212 (B)

Z.-X. Shen and Schrieffer, PRL **78**, 1771 (1997)

2. The interplane hopping $t_{\perp} \propto (\cos k_x - \cos k_y)^2$ vanishes at the “cold spots”, where $k_x = \pm k_y$ (Liechtenstein, Gunnarson, O. K. Andersen and Martin, Phys. Rev. B **54**, 12505 (1996)). Thus, the c -axis resistance ρ_c is determined by the “hot” regions, whereas the ρ_{ab} is controlled by the “cold spots”.

Extreme "cold spots" model

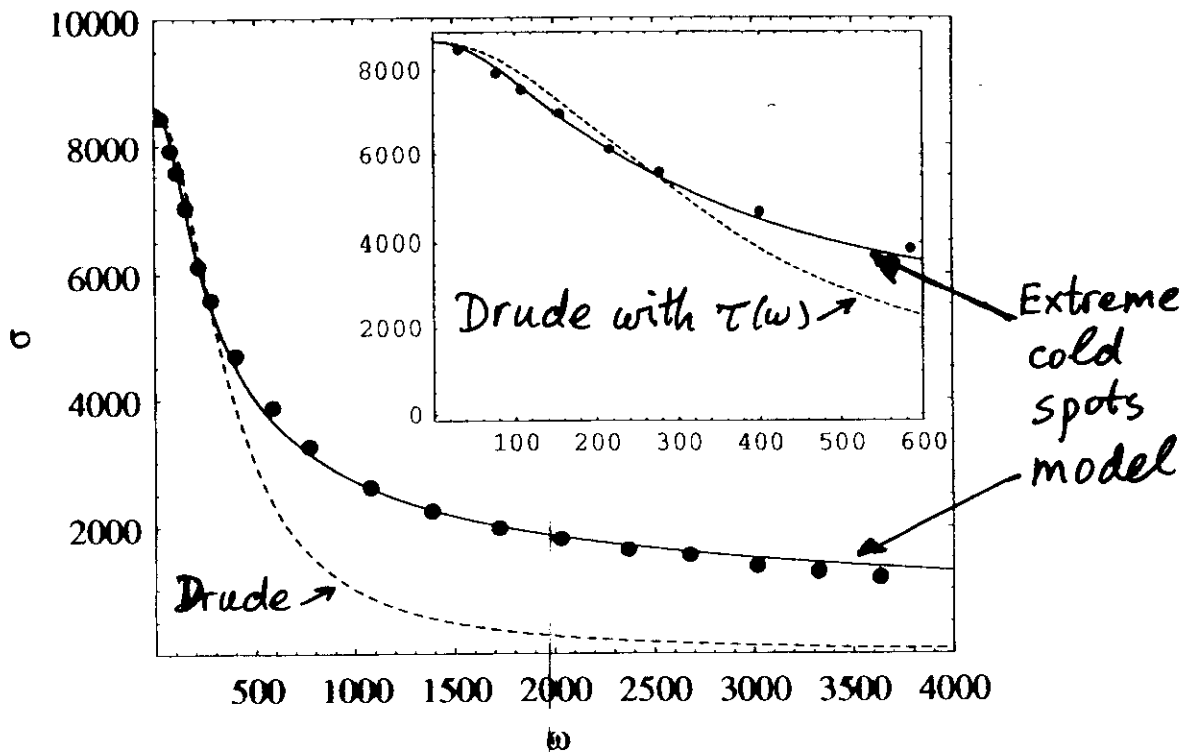
Ioffe & Millis, cond-mat/9801092, January 1998

PRB 58, 11631 (1998)

$$\begin{aligned}\sigma_{xx}(\omega) &\propto \int \frac{dk_t}{-i\omega + 1/\tau(k_t)} \approx \int \frac{dk_t}{-i\omega + 1/\tau_0 + \Gamma k_t^2} \\ &\propto \frac{1}{\sqrt{\Gamma}} \sqrt{\frac{\tau_0}{1 - i\omega\tau_0}} \propto \frac{1}{T} \propto \frac{1}{\sqrt{-i\omega}}\end{aligned}$$

$1/\tau_0 \propto T^2$ is the relaxation rate at the cold spot.

Γ is temperature independent.



Data (●): Orenstein et al., Phys. Rev. B **42**, 6342 (1990).

Magnetotransport in the model of Ioffe and Millis

$$\sigma_{xy}(\omega) \propto \int \frac{dk_t}{(-i\omega + 1/\tau(k_t))^2} \propto \left(\frac{1}{1/\tau_0 - i\omega} \right)^{3/2}$$

$$\cot \theta_H(\omega) = 1/\tau_0 - i\omega, \quad 1/\tau_0 = 7 \text{ meV}$$

$\cot \theta_H(\omega)$ agrees with the experiment by Kaplan
et al. ~~but not the data of~~ **Grayson, 2000**

Problems, open questions

- $\frac{1}{\tau}$ from photoemission is not $\propto T^2$ and is substantially bigger than in transport
- Quasiparticles are not well-defined (abnormal EDCs)
- Not clear how to obtain $\frac{1}{\tau} \sim \text{const}$, T , $\frac{T^2}{T_0}$ from a microscopic theory on different parts of the Fermi surface
- $T_0 \sim 120\text{K}$ is too small for a Fermi liquid (should be E_F , at least)
- $\frac{1}{\tau_H} \propto T^2$, but not $(T^2 + \omega^2)$ Černe PRL 2000

Conclusions

Transport models with a variation of τ over the Fermi surface (cold spots models) work reasonably well, but there are open questions.

Models of the normal-state transport in high- T_c superconductors

$$\frac{1}{\tilde{\tau}(\omega)} = \frac{1}{\tau} - i\omega$$

	Experiment	Drude	Additive two- τ	Ioffe Millis	Anderson	Coleman Schofield Tsvelik
<i>van der Marel</i>						
σ_{xx}	$1/T$	$\tilde{\tau}$	$A_1 \tilde{\tau}_1 + A_2 \tilde{\tau}_2$	$\sqrt{\tilde{\tau}_0} \sqrt{\tilde{\tau}'}$	$\tilde{\tau}_{tr}$	$\tilde{\tau}_f \tilde{\tau}_s / (\tilde{\tau}_f + \tilde{\tau}_s)$
σ_{xy}	$1/T^3$	$\tilde{\tau}^2$	$A_1 \tilde{\tau}_1^2 + A_2 \tilde{\tau}_2^2$	$\tilde{\tau}_0^{3/2}$	$\tilde{\tau}_{tr} \tilde{\tau}_H$	$\tilde{\tau}_f \tilde{\tau}_s$
$\sqrt{\tilde{\tau}_0 \tilde{\tau}' / (\tilde{\tau}_0 + \tilde{\tau}')}$						
			$1/\tau_1 \propto T$		$1/\tau_{tr} \propto T$	$1/\tau_f \propto T$
			$1/\tau_2 \propto T^2$	$1/\tau_0 \propto T^2$	$1/\tau_H \propto T^2$	$1/\tau_s \propto T^2$

$$\frac{1}{\tilde{\tau}'} = \frac{1}{\tilde{\tau}_0} + \frac{1}{\tilde{\tau}_s}$$